

MODELLING THE ELECTROTONIC STRUCTURE OF STARBURST AMACRINE CELLS IN THE RABBIT RETINA: A FUNCTIONAL INTERPRETATION OF DENDRITIC MORPHOLOGY

■ ROMAN R. POZNANSKI*
Centre for Visual Sciences,
Research School of Biological Sciences,
Australian National University,
Canberra, ACT 2601, Australia

A detailed morphometric analysis of a Lucifer yellow-filled Cb amacrine cell was undertaken to provide raw data for the construction of a neuronal cable model. The cable model was employed to determine whether distal input–output regions of dendrites were electrically isolated from the soma and each other. Calculations of steady state electrotonic current spread suggested reasonable electrical communication between cell body and dendrites. In particular, the centripetal voltage attenuation revealed that a synaptic signal introduced at the distal end of the equivalent dendrite could spread passively along the dendrite and reach the soma with little loss in amplitude. A functional interpretation of this result could favour a postsynaptic rather than a presynaptic scheme for the operation of directional selectivity in the rabbit retina. On the other hand, dendrites of starburst amacrine cells process information electrotonically with a bias towards the centrifugal direction and for a restricted range of membrane resistance values the voltage attenuation in the centripetal direction suggests that the action of these dendrites can be confined locally. A functional interpretation of this result favours a presynaptic version of Vancay's cotransmission model which attempts to explain how the neural network of starburst amacrine cells might account for directionally selective responses observed in the rabbit retina.

Introduction. The classical electrophysiological experiments undertaken by Barlow and colleagues (Barlow and Hill, 1963; Barlow *et al.*, 1964; Barlow and Levick, 1965; Oyster and Barlow, 1967) exposed the underlying mechanisms by which certain ganglion cells in the rabbit retina respond preferentially to the direction of visual motion, but in the 26 years since the publication of Barlow and Levick's classic description of the mechanism of direction-selectivity the cellular basis of its operation still remains to be completely understood.

However, detailed anatomical studies of the inner plexiform layer in several vertebrate retinas (Dowling, 1968; Dowling and Werblin, 1969) led Dowling to propose a scheme of how directionally selective responses could be mediated in the inner plexiform layer by amacrine cells (Dowling, 1970). This scheme incorporates the main anatomical features found in retinas of those vertebrate

* Present address: Neurobiology Research Centre and School of Mathematics, Carlsaw Building F07, The University of Sydney, NSW 2006, Australia.

species having directionally selective ganglion cells. A reader not familiar with the neuronal network of cells in the mammalian retina may wish to consult the monograph by Dowling (1987) or a recent review article by Wassle and Boycott (1991) for an overview.

The biophysical mechanism for implementing directional selectivity was shown by Dowling to involve the interaction between an excitatory and inhibitory input at the level of the amacrine-ganglion cell synapse. Nevertheless, such a scheme allows just one kind of amacrine cell to do too much. For example, opposite sides of the amacrine's dendritic tree connect to the same ganglion cell which is unnecessarily complex. Therefore, regardless of its success in pinpointing the retinal location of direction-selective interactions and the nature of these neural interactions, the Dowling model, having several caveats in its topological layout, needs to be modified before it can begin to explain the mechanisms governing direction-selectivity and in particular, the spatial organization of direction-selectivity. A modification of the Dowling model is schematically illustrated in Fig. 1.

The topology of the modified Dowling model as illustrated in Fig. 1 is able to account for the multiplicity of directionally selective subunits and also the existence of an "inhibition-free" zone adjacent to the edge of the receptive field that is first crossed when motion is in the preferred direction (Barlow and Levick, 1965). Note that although only a single layer is shown in Fig. 1, a bistratified dendritic field is required with one stratum in each of the ON and OFF layers and also the synaptic mechanism associated with a single subunit should be repeated many times, but here it is highly magnified in order to show off the synaptic arrangements.

In the modified Dowling model the nominated amacrine cells could be two quite different types of cells, but a more recent model incorporating the pharmacological data (Masland and Ames, 1976; Wyatt and Daw, 1976; Caldwell *et al.*, 1978; Ariel and Daw, 1982) which has identified the transmitters ACh (acetylcholine) and GABA (γ -aminobutyric acid) in the generation of ON-OFF directionally selective responses and hence identified the type of amacrine cells involved in the operation of direction-selectivity has recently been outlined by Vaney (see Vaney *et al.*, 1989; Vaney, 1990).

The major proposition of Vaney's model is based on the idea that ACh is released onto a specific directionally selective ganglion cell only from segments of starburst amacrine* whose distal tips are located on the side of the amacrine field which is first stimulated by movement in the null direction (Vaney *et al.*, 1989; Vaney, 1990)†. Assuming that the major proposition of the model holds

* Only the outer varicose region of each dendrite represents the output zone to an overlaying directionally selective unit (Famiglietti, 1983b, 1985).

† This premise is rather speculative and it is currently being investigated from a physiological point of view by W. R. Levick, FRS and D. I. Vaney in a jointly funded project.

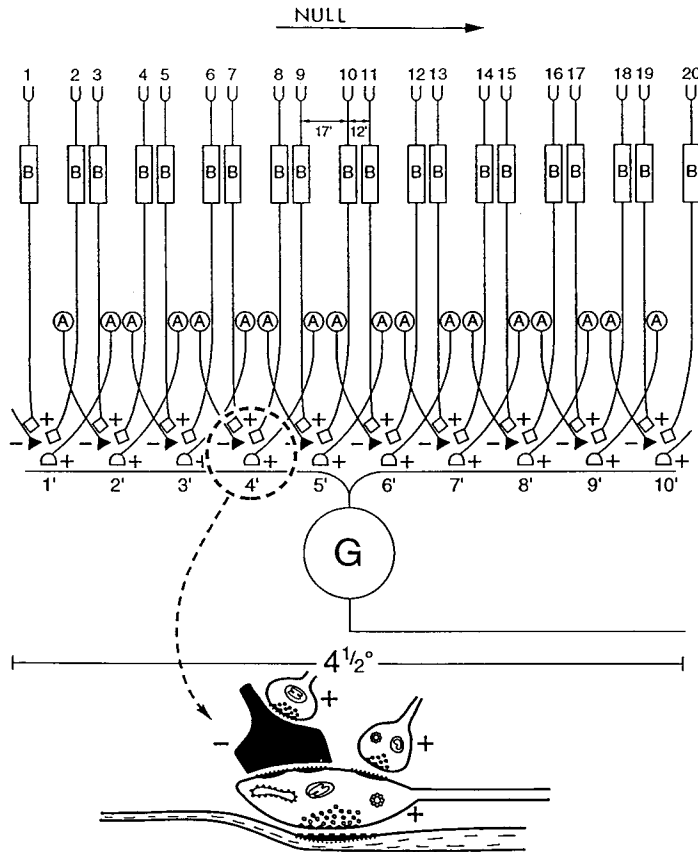


Figure 1. The anatomical structure of the model consists of a directionally selective ganglion cell with a receptive field subtending $4\frac{1}{2}^\circ$ and sequence-discriminating subunits made up from the distal dendrites of starburst amacrine cells activated by bipolar cells. The inhibitory mechanism for implementing the sequence-discrimination corresponding to a single subunit is shown to be excited by bipolar inputs whose cell bodies are 17' apart, while successive subunits are separated by bipolar inputs whose cell bodies are 12' apart. This is in agreement with the single-slit experiment, whereby the complete mechanism of directional selectivity was found to be contained within a small subunit 1/9 to 1/18 of the entire receptive field (see Barlow and Levick, 1965). The existence of an "inhibition-free" zone adjacent to the edge of the receptive field that is first crossed when motion is in the preferred direction extends approximately $\frac{1}{4}^\circ$ from the edge. A serial synapse is shown enlarged with (+) denoting an excitatory synapse and (-) an inhibitory synapse. The serial synapses are arranged such that an amacrine-amacrine synapse uses GABA to inhibit the amacrine-ganglion cell synapse. With the serial synapses organized as in the diagram, a spot moving from left to right (null direction) will result in no firing in the ganglion cell. (A) denotes starburst amacrine cells; (B) denotes cone bipolar cells; (G) denotes a directionally selective ganglion cell. (Modified from Dowling, 1970.)

then the following corollaries are essential if a *presynaptic* version of Vaney's cotransmission model is to be considered valid.

(1) Segments of starburst amacrine cells located in other quadrants would provide ACh input to directionally selective ganglion cells with different preferred directions (Vaney, 1985, 1990; Vaney *et al.*, 1989).

(2) Ganglion cells which respond to different preferred directions receive synaptic input from different segments of the starburst amacrine cells. This prevents the co-release of GABA and ACh from occurring,* since overlapping receptive fields of any two directionally selective units rarely have identical preferred directions.

(3) Asymmetric ACh input to directionally selective ganglion cells is in turn symmetrically inhibited from all segments of starburst amacrine cells (Vaney *et al.*, 1989; Vaney, 1990).

The model shown in Fig. 2 does in fact explain the topographic physiological features of directional selectivity by illustrating the essential relationship between directionally selective ganglion cells and starburst amacrine cells. For example, the model as shown in Fig. 2b can account for the distribution of silent-inhibition around a local region (subunit) in the receptive field of a single directionally selective unit. It is known that starburst amacrine cells receive a sparse distribution of bipolar inputs over their entire dendritic tree (Famiglietti, 1983b, 1991) with the area of distribution of these inputs resembling a cardioid shape, compatible with the physiological observations of Wyatt and Daw (1975). Therefore, these bipolar cell inputs have a significant role in initiating the release of GABA from the "output" zone (i.e. the dendritic terminal area) of each starburst amacrine cell on to a directionally selective ganglion cell.

The *physiological* definition of a subunit is the smallest distance a stimulus must be moved in order to elicit a directionally selective response, which is approximately 17' or 30 μm in linear distance on the retina (Barlow and Levick, 1965). In the model the *morphological* definition of the subunit is the aggregate of dendritic terminals of overlapping starburst amacrine cells which constitute about one or two lattice units roughly 20–30 μm wide, supporting the anatomical measurements made by Brandon (1987), and are assumed to follow the looping morphology of the ON-OFF direction-selective unit as observed by Amthor *et al.* (1984).

The model assumes the existence of starburst–starburst connections together with the release of ACh and GABA from these cells upon visual stimulation. The colocalization assumption allows for just one type of amacrine cell to mediate both the excitation and inhibition. There exists morphological evidence that starburst processes interact synaptically with

* The release sites for GABA and ACh are co-distributed within the varicose annular zone covering the distal dendrites of each starburst amacrine cell.

each other (Millar and Morgan, 1987). Furthermore, it has been recently discovered that the starburst amacrine cells store (Vaney and Young, 1988) and synthesize (Brecha *et al.*, 1988) GABA. There is strong evidence for the role of ACh as a transmitter used by starburst amacrine cells because cholinergic enzymes (e.g. choline acetyltransferase) are present in these cells and also because ACh is known to be released during light stimulation (Masland and Ames, 1976). However, the identification of GAD (glutamate decarboxylase) does not imply with certainty that GABA is used as a transmitter, because it has been shown that GABA is released from starburst amacrine cells through a carrier system that is insensitive to light stimulation (O'Malley and Masland, 1989). It may be that both ACh and GABA release is modulated by light but ACh release being highly amplified.

The model also assumes that a GABA releasing amacrine cell is presynaptic to an ACh releasing amacrine cell, which appears to be very likely, since Massey and colleagues (Massey and Neal, 1979; Neal and Massey, 1980;

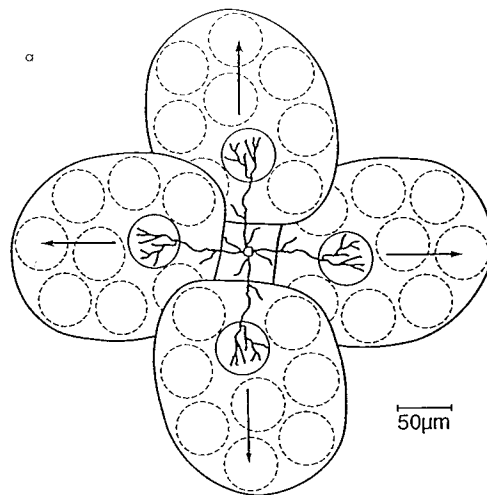


Figure 2a. The model predicts that a single amacrine cell provides excitatory input to directionally selective subunits from four different groups of ganglion cells whose preferred directions are anisotropic with respect to each other. The mechanism of direction-selectivity is contained within a single subunit that is reduplicated nine or more times to cover the total area of a particular receptive field in agreement with the physiological observations of Barlow and Levick (1965). The receptive field of each directionally selective unit is shown to possess a preferred direction that is restricted to one of four non-overlapping directions observed by Oyster (1968) (see also Oyster and Barlow, 1967). Each individual direction-selective ganglion cell is shown to have the same direction of preferential response (indicated by arrow) throughout its receptive field in accordance with the experimental results (see Barlow and Hill, 1963; Barlow *et al.*, 1964).

Massey and Redburn, 1982) have shown that GABA appears to modulate the release of ACh suggesting the presence of GABAergic input onto the cholinergic amacrine cells. Regardless of the presumed existence of GABAergic synapses impinging directly upon directionally selective ganglion cells (Famiglietti, 1985), the model assumes that GABA receptors are found only on

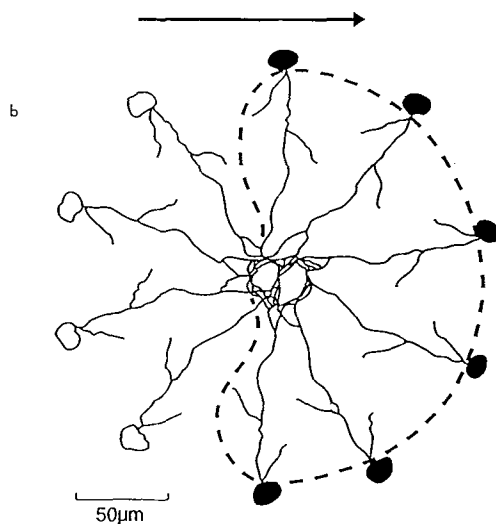


Figure 2b. The model proposes that any chosen local region (subunit) in the receptive field of a single directionally selective unit receives input from the distal dendrites of starburst amacrine cells. In other words the "output" zone for GABA and ACh release is restricted to the dendritic terminals of starburst amacrine cells. The dendrites of starburst amacrine cells with somata shown as unfilled circles provide cholinergic input to the chosen subunit, while the dendrites which mediate the release of GABA are spatially arranged so as to produce a "silent" inhibitory surround (shown by the dashed line) that is similar in appearance to the cardioid shape observed experimentally by Wyatt and Daw (1975). In accordance with the two spot experiments, the lateral extent of this inhibitory area is just under half the size of the receptive field diameter of the directionally selective ganglion cell and it can also project some distance into the surround of the receptive field, depending on the position of the local region (subunit) in the receptive field (see Wyatt and Daw, 1975). Furthermore, given that the directionally selective unit has a receptive field slightly greater than the dendritic field of a starburst amacrine cell at each eccentricity, the silent-inhibitory surround should extend for only half the width of a starburst amacrine cell (Vaney, 1990; Vaney *et al.*, 1989). The size of the silent inhibitory surround would be dependent on the eccentric placement of the starburst amacrine cell with respect to the visual streak in rabbit or *area centralis* in cat. For example, in the visual streak the dendritic field diameters are in the range of 250 μm , while in the peripheral retina they range up to 800 μm , suggesting a large variation with retinal eccentricity (see Tauchi and Masland, 1984). The preferred direction of the directionally selective unit encompassed by the network of starburst amacrine cells is shown by the arrow. (Modified from Vaney, 1990.)

cholinergic amacrine cells, while ACh receptors are restricted to the direction-selective ganglion cells.*

If the model is to remain operational the dendrites of starburst amacrine cells will need to be electrically isolated from each other. Otherwise, inhibition induced by movement in the null direction for a particular quadrant of the starburst amacrine cell could prevent the release of ACh from another quadrant, whose motion was in the preferred direction, thereby producing an alternating pattern of excitation and inhibition in the null direction. Furthermore, the GABA releasing amacrine cells require effective electrical communication throughout their dendritic tree, especially in the centrifugal direction in order to explain the existence of the cardioid inhibitory spread driven by the sparse distribution of bipolar inputs onto the starburst amacrine cells. Therefore, if the starburst amacrine cells are cholinergic as well as GABAergic then the flow of axial current along dendrites in the centrifugal direction must be "reasonable", while "poor" in the centripetal direction [cf. Oyster, 1989 (Fig. 9.7)].

The use of one-dimensional cable theory and morphological data obtained under light microscopy of a Lucifer-yellow filled starburst amacrine cell will need to be undertaken in order to determine whether the local direction-sensitive electrical action in one dendritic peripheral bush can be confined locally and more importantly, whether dendrites of starburst amacrine cells process information with a bias towards the centrifugal direction.

In Golgi-impregnated and dye-injected material the starburst amacrine cells in the rabbit retina show an unusual dendritic architecture that includes thin intermediate dendritic segments (Famiglietti, 1983a; Miller and Bloomfield, 1983), and varicosities confined to the more distal branches which serve as input-output sites via dendrodendritic synapses.

On the basis of cable modelling, Miller and Bloomfield (1983) suggested that the distal dendrites of starburst amacrine cells might be electrically isolated from the soma due to the presence of the intermediate zone of thin dendrites. The computations undertaken by Miller and Bloomfield (1983) using a passive steady-state cable model (Rall, 1959) revealed that input to a varicosity in the periphery would decay over a relatively short electrotonic distance and contribute ($< 10\%$) to the voltage at the soma. In particular, if the diameter of the primary branch conformed to the $3/2$ power-law of Rall then it was shown that in the centripetal direction the voltage attenuated to about 10.6% of its initial value, while in the centrifugal direction to approximately 88.6% of its initial value. These results imply that starburst amacrine cells consist of subunits functioning as electrically independent local input-output circuits and that the operational unit in the starburst network is not the whole cell but

* This assumption requires further analysis and is currently underway in the laboratory of I. G. Morgan (see for example, Morgan and Li, 1990).

rather a segment of its dendritic arbor. This hypothesis is important because these anatomical segments have the right size and shape to account for the direction-selective subunits in the receptive fields of ganglion cells reported by Barlow and Levick (1965) (see Oyster, 1989; Vaney, 1990; Borg-Graham and Grzywacz, 1992; for an overview).

However, the analysis of Miller and Bloomfield is open to criticism as it was limited to the steady-state, and more importantly was dependent upon the assumption of a constant and uniform value of $4\,000\ \Omega\text{cm}^2$ for the specific membrane resistivity (R_m) of the dendritic surface. The omission of capacitance can be justified by the slow time-course of most of the inputs to the starburst amacrine cells. For example, it is known that cone bipolar responses are "sustained" and anatomical evidence provided by Famiglietti (1983b, 1991) shows that cone bipolar inputs are distributed throughout the dendrites of starburst amacrine cells. On the other hand, to the best of my knowledge there are no estimates of the electrical parameters of starburst amacrine cells and therefore, it is clearly premature to suggest any kind of electrotonic model based on parameters commonly associated with other mammalian neurons. Nevertheless, some references to electrical parameters of amacrine cells in general have been made by Nelson (1973) and more recently by Coleman and Miller (1989) from cold-blooded lower vertebrates. Nelson (1973) suggested an average R_m of the soma to be in the range $1\,000\text{--}3\,000\ \Omega\text{cm}^2$ with an axial resistivity (R_i) of $300\ \Omega\text{cm}$ (assuming negligible extracellular resistivity), while Coleman and Miller (1989) have suggested an average R_m of $68\,000\ \Omega\text{cm}^2$. However, there may be a serious hazard in inferring the properties of mammalian neurons from those of lower vertebrates, but these values indicate that the electrical parameters chosen by Miller and Bloomfield (1983) may have been too low by a factor of 10 or more.

Furthermore, in electrophysiological studies of mammalian CNS neurons, the uniform R_m assumption in most situations overestimates the accepted value of $C_m = 1\ \mu\text{F}/\text{cm}^2$ for biological membranes (Cole, 1968). One way to resolve this problem has been to assume a monotonically increasing R_m distribution (Rall, 1982; Fleshman *et al.*, 1988). This assumption deserves more attention as it is highly probable that starburst amacrine cells undergo constant synaptic bombardment throughout their dendritic arbor, especially in the periphery increasing the membrane conductance in a non-uniform manner. Although electrophysiological experiments on starburst amacrine cells have not yet been undertaken, in general, synaptic inputs alter ionic conductance which can lower the measured R_m from its resting value during recording. To compensate for the lower measured R_m due to such synaptic activity (which in many cells may be concentrated on peripheral dendrites), the value of R_m may increase with distance from the soma in a monotonic fashion. Therefore, one aim of this paper will be to test the robustness of the Miller and Bloomfield (1983) results

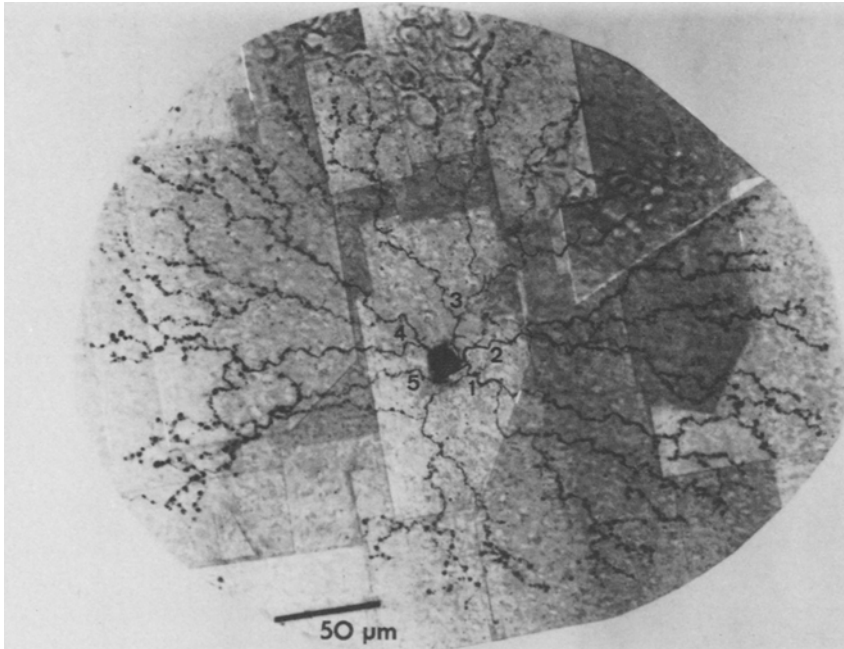


Figure 3. A flat-mount micrograph of a Lucifer yellow-filled Cb (off-type) starburst amacrine cell used as a specimen in the morphometric analysis. The numbers correspond to the "dendrite number" specified in Table 1 (calibration bar represents 50 μm).

by varying the R_m assumption,* keeping in mind the functional implication behind such an analysis.

Experimental Methods. A single Cb amacrine cell from the visual streak of the rabbit retina was kindly provided by Dr D. I. Vaney (VTHRC, University of Queensland). The cell was injected with the fluorescent dye Lucifer-yellow, and after fixation the dye was converted to an opaque product by photo-oxidation in the presence of DAB. This procedure allows direct visualization of the Lucifer-yellow filled cell under light (see Maranto, 1982; Vaney, 1984, for details on the Lucifer-DAB staining procedures).

In order to perform a morphometric analysis of the labelled cell a series of micrographs were taken under an overall total magnification of $\times 1000$ using a Zeiss photomicroscope II. A montage of the amacrine cell is shown in Fig. 3.

The diameter and length of each dendritic branch segment was measured using a $\times 400$ oil-immersion objective lens and a micrometer-driven filar eyepiece. The diameters of beaded dendritic segments were estimated by measuring the diameters of the beaded and constricted regions and calculating a weighted average. In most cases, an average diameter was calculated from measurements made at every $5\ \mu\text{m}$. A resolution of $0.3\ \mu\text{m}$ was assumed and no attempt was made to adjust measurements by a scaling factor as a result of fixation and dehydration. The results are tabulated below (see Table 1) with the five dendrites of the Lucifer-filled starburst amacrine cell drawn as binary dendrograms in terms of anatomical path distance (see Fig. 4).

The dendritic branches were divided into individual segments each represented by a smooth cylinder of uniform diameter. The diameter and length of each segment was then used in calculating the membrane surface area of the dendritic segment. The membrane surface area of all five dendrites yielded the total membrane surface area calculated in successive $10\ \mu\text{m}$ distance bins (Fig. 5). The cumulative membrane surface area scaled as per cent of total membrane surface area was also determined with the curve shown in Fig. 5. This curve was used as an initial guide to the assumed non-uniformity in R_m —a procedure used by Fleshman *et al.* (1988) for cat motoneurons.

The actual R_m values attached to this curve were chosen from a postulated soma resistivity of $1\ 000\ \Omega\text{cm}^2$ (Nelson, 1973), increasing to a final value of $R_{m,\text{max}}$. For each segment an average (or mean) R_m value was selected from a section of the curve corresponding to the physical distance from the soma of the particular branch element. This enabled the electrotonic length of an individual branch to be determined from the well-known equation:

$$l/\sqrt{(R_m d/4R_i)} \quad (1)$$

* At present this assumption remains purely theoretical. However, there may be a way to experimentally test whether R_m is spatially non-uniform (e.g. to investigate the behaviour of the neuron after a voltage perturbation, see Fleshman *et al.*, 1988; or to use voltage sensitive dyes, see Tsien, 1989).

Table 1

Dendrite number/ branch order	Length (μm)	Diameter (μm)	Dendrite number/ branch order	Length (μm)	Diameter (μm)
11	11	0.74	34	36	0.42
12	31	0.44	34	41	0.42
12	19	0.83	34	62	0.83
13	106	0.69	34	27	1.02
13	22	0.37	34	30	0.88
13	44	0.42	35	26	0.69
13	100	0.74	35	78	0.83
14	43	0.68	35	51	0.42
14	60	1.17	35	50	0.35
14	62	0.33	35	39	0.80
14	89	0.89	35	50	0.83
14	62	0.83	35	44	0.83
14	60	0.90	35	17	0.65
14	21	0.56	35	37	0.83
14	69	1.10	35	11	0.56
15	19	0.49	36	53	0.72
15	23	1.11	36	48	0.65
15	46	1.11	36	15	0.97
15	7	0.97	36	6	0.83
15	46	0.75	36	9	0.56
15	61	0.74	36	14	0.83
15	14	1.11	41	6	0.97
15	27	1.17	42	31	0.61
16	38	0.90	42	126	0.59
16	27	0.63	43	59	0.78
16	36	1.22	43	57	0.75
16	33	0.84	43	22	0.69
16	34	1.28	43	15	0.83
16	18	1.02	44	23	0.67
16	10	1.39	44	56	0.79
16	18	0.93	44	39	0.56
21	43	0.66	44	35	0.42
22	77	0.73	44	32	0.50
22	37	0.74	44	12	0.83
23	99	0.72	45	12	0.83
23	37	0.97	45	37	1.17
23	63	0.83	45	26	0.65
23	41	1.03	45	14	0.84
24	6	0.74	45	44	0.79
24	43	0.73	45	35	0.84
24	48	0.97	45	57	0.69
24	19	1.46	45	33	0.61
24	42	0.75	45	35	1.00
24	74	0.91	45	21	0.46
25	33	1.11	46	11	0.56
25	24	1.04	46	26	1.83
25	22	1.46	46	16	0.65
25	26	1.22	46	32	1.04
31	22	0.37	46	12	0.83
32	22	0.28	46	16	0.83
32	64	0.51	51	79	0.42
33	31	0.42	52	14	0.83
33	50	0.52	52	66	0.49
33	23	0.61	53	14	1.16
33	97	0.79	53	6	0.83
34	93	0.49	54	27	0.56
			54	21	1.11



Figure 4. Dendrograms of five dendrites from the Cb starburst amacrine cell (see Fig. 3) plotted in terms of anatomical path distance from the cell body (abscissa). Each horizontal line represents a dendritic branch. The thickness of each horizontal line represents the average diameter of the branch (calibration bar on lower left represents 1.2 μm).

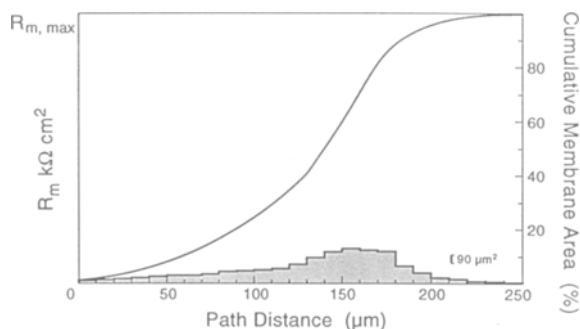


Figure 5. A curve showing the assumed sigmoidal R_m increase (left ordinate) and the cumulative membrane area (right ordinate, scaled as per cent of total area) both plotted as functions of dendritic path distance (abscissa). The cell body area was omitted from the calculations. Histogram of membrane areas in successive $10\ \mu\text{m}$ bins is shown at bottom (calibration bar on lower right represents $90\ \mu\text{m}^2$).

where a different diameter (d), length (l) and specific membrane resistivity (R_m) for each segment, but a common value for the axial specific resistivity (R_i) of $300\ \Omega\text{cm}$ was assumed (Nelson, 1973). The total electrotonic length along a dendritic path from the soma to the point of measurement was obtained as the sum of all the electrotonic lengths of the individual branch segments. It should be mentioned that in some cases, R_m values were adjusted slightly ($< 5\%$) in order for dendrites to terminate at identical electrotonic distances from the soma—a condition required for the reduction of the dendritic tree into an equivalent cable (Rall, 1962). A larger class of dendritic tree patterns with branch segments terminating at unequal electrotonic distances from the soma could also be treated by the cable model, but only if it was also assumed that end effects from dendrites terminating at different electrotonic distances from the soma were negligible, as would be the case when viewed from the soma.

Mathematical Model. The steady state voltage decrement in a dendritic neuron having a complex branching pattern can be found by the iterative method devised by Rall (1959), or by the method outlined by Rall and Rinzel (1973) where use is made of symmetry arguments to quickly derive solutions for neurons with idealized branching conditions. Although these models are extremely useful they assume that R_m is uniform over the entire dendritic surface, which has been questioned recently by several authors (see Rall, 1982; Redman *et al.*, 1987; Fleshman *et al.*, 1988; Holmes and Woody, 1989; Pongracz *et al.*, 1991).

An alternative approach is to generalize the equivalent cable model originally developed by Rall (1962) or the more recent equivalent cable model developed by Poznanski (1991) to obtain the equation under which a dendritic tree with complex geometry and spatially non-uniform R_m can be collapsed

into a single equivalent cable, and henceforth solve analytically the equation governing the steady state decrement of voltage in such a non-uniform structure. It should be mentioned that numerical algorithms (see for example, Hines, 1989) employed in compartmental models of neurons with different R_m values in each branch segment is an alternative approach that will not be discussed here (see Rall, 1990, for a critical analysis of this technique with regard to the problem of non-uniqueness).

The aim of this section will be to generalize the condition for reduction to a geometrically tapering equivalent cable (see for example, Rall, 1962; Goldstein and Rall, 1974; Poznanski, 1988, 1991) to include electric non-uniformities such as a spatially non-uniform R_m distribution. The derivation will be carried out in the steady-state domain, but extension to the time-dependent domain can be carried out along the same lines as sketched by Leibovic (1972) for a symmetrical tree.

The steady-state voltage distribution in a dendritic tree with cylindrical branches is known to be governed by the following ordinary differential equation [cf. Rall, 1962, equation (17); Jack *et al.*, 1975, equation (7.40)]:

$$[r(x)R_m(x)/2R_i]\left(\frac{dZ}{dx}\right)^2\left\{\frac{d^2V}{dZ^2} + \frac{dV}{dZ}\left(\frac{dZ}{dx}\right)^{-1} \frac{d}{dx} \ln\left[r^2(x)n(x)\frac{dZ}{dx}\right]\right\} = V \quad (2)$$

where the radius (r) of all branch segments, the number of dendritic branches (n) and R_m are all functions of actual distance (x) from the soma (assumed to be the point $x=0$). The variable Z is defined as:

$$Z = \int_0^x \lambda_{\text{taper}}^{-1} d\zeta \quad (3)$$

which defines the electrotonic distance for situations where there is a continuously changing characteristic length parameter (λ_{taper}):

$$\lambda_{\text{taper}} = [R_m(x)r(x)/2R_i]^{1/2} \quad (4)$$

where R_i is the axial resistivity assumed to be constant. The basis for these equations can be found in earlier work (see Rall, 1962; Goldstein and Rall, 1974; Poznanski, 1988, 1991).

Likewise, the general equation for steady-state voltage distribution in a single one-dimensional uniform cable has the following form (Jack *et al.*, 1975, p. 148):

$$\frac{d^2V}{dX^2} = V. \quad (5)$$

The aim will now be to relate equation (5) to equation (2) by some kind of

power law. Integrating equation (3) with respect to x and substituting the result into equation (2) yields the following expression:

$$\frac{d^2 V}{dZ^2} + \frac{dV}{dZ} [R_m(x)r(x)/2R_i]^{1/2} \frac{d}{dx} \ln[r^{3/2}(x)n(x)/R_m^{1/2}(x)] = V \quad (6)$$

which will reduce to equation (5) only if the coefficient of dV/dZ is set equal to zero. Neither $r(x)$ or $R_m(x)$ can be zero for any realizable structure and therefore, the only condition becomes:

$$n(x)r^{3/2}(x)R_m^{-1/2}(x) = n(0)r^{3/2}(0)R_m^{-1/2}(0) \quad (7)$$

where $r(0)$ is the radius, $R_m(0)$ is the specific membrane resistivity and $n(0)$ is the number of branches all defined at the point $x=0$.

If for convenience each branch segment at any given value of x is characterized by a different diameter and $R_m(x)$ [as branch segments may extend over a range of x values a mean value of $R_m(x)$ is taken for each branch segment to ensure that within a segment $R_m(x)$ is fixed], and branching occurs at distances $0 = x_0 < \dots < x_p$ with n_i branches between x_i and x_{i+1} where $x_i \leq x \leq x_{i+1}$ then after replacing radius with diameter, together with the above assumptions equation (7) becomes:

$$\sum_{j=1}^{n_i} (d_{ij}^3/R_{mij})^{1/2} = \sum_{j=1}^{n_0} (d_{oj}^3/R_{moj})^{1/2} \quad i=0, 1, \dots, p \quad (8)$$

which is identical to equation (7.23) in Jack *et al.* (1975) when R_i is constant.

If equation (8) holds at every given electrotonic distance from the soma and all terminal branches end at the same electrotonic distance from the soma (with all terminations having the same boundary condition) then the tree can be transformed mathematically into an equivalent cylinder and the steady-state voltage distribution determined from equation (5) with Z replaced by X .

However, if for a particular neuron under investigation equation (8) does not hold then a parameter F can be introduced which would approximate the profile followed by equation (8) at a given electrotonic distance from the soma:

$$F(Z) = \left(\sum_{j=1}^{n_i} d_{ij}^{3/2} \right) / \left(\sum_{j=1}^{n_0} d_{oj}^{3/2} \right) \left(\sum_{j=1}^{n_0} R_{moj}^{1/2} \right) / \left(\sum_{j=1}^{n_i} R_{mij}^{1/2} \right). \quad (9)$$

It should be noted that the parameter F produce a non-uniformity in the equivalent cable that is both geometrical and electrical. With the substitution of parameter F into equation (6) the resultant expression can be shown to reduce to the following modified cable equation:

$$\frac{d^2 V}{dZ^2} - V + F^{-1} \frac{dF}{dZ} \frac{dV}{dZ} = 0 \quad (0 < Z < L) \quad (10)$$

representing voltage distribution in a one-dimensional tapering structure of electrotonic length (L)-defined as the sum of all branch lengths encountered each divided by a characteristic length parameter for that particular branch element. Defining L for a tree with dendrites ending at unequal electrotonic distances is beyond the scope of this paper (but see Glenn, 1988, for an interpretation of the electrotonic length associated with a non-uniform equivalent cable model).

The determination of the steady-state voltage decrement with electrotonic distance along a non-uniform equivalent cable can be obtained once a complete boundary value problem (BVP) has been set up for solving. For voltage attenuation in the centripetal direction the boundary conditions $V_z(0)=0$ and $V(L)=V_{in}$, together with equation (10), define the complete BVP to be solved. Likewise, for voltage attenuation in the centrifugal direction the boundary conditions $V(0)=V_{in}$ and $V_z(L)=0$, together with equation (10) define the complete BVP to be solved. After performing some tedious algebra it can be shown that the solution of equation (10) for the specific case of voltage decrement from the distal-end to the soma (centripetal direction) along the non-uniform equivalent cable is given by equation (6.4) derived in Poznanski (1990). Likewise, the voltage decrement from the soma to the distal-end (centrifugal direction) of the non-uniform equivalent cable is given by equation (6.5) derived in Poznanski (1990).

As an illustrative example consider the voltage attenuation along a tapering (exponentially) equivalent cable. Here the "electrogeometric" ratio factor $F(Z)$ is approximated by an exponential function $\exp(KZ)$ where ($K < 0$) is a constant controlling the amount of taper present, and after performing some tedious algebra it can be shown that the voltage decay from the distal-end to the soma of the exponentially tapering equivalent cable is given by the following result:

$$\begin{aligned} V/V_{in} = \exp[\tfrac{1}{2}K(L-Z)] \{ & (\sqrt{(1+\tfrac{1}{4}K^2)} \cosh \sqrt{(1+\tfrac{1}{4}K^2)}Z \\ & + \tfrac{1}{2}K \sinh \sqrt{(1+\tfrac{1}{4}K^2)}Z) / (\sqrt{(1+\tfrac{1}{4}K^2)} \cosh \sqrt{(1+\tfrac{1}{4}K^2)}L \\ & + \tfrac{1}{2}K \sinh \sqrt{(1+\tfrac{1}{4}K^2)}L) \} \end{aligned} \quad (11)$$

and the decay of voltage from the soma to the distal-end of the exponentially tapering equivalent cable is given by the following result:

$$\begin{aligned} V/V_{in} = \exp[-\tfrac{1}{2}KZ] \{ & (\sqrt{(1+\tfrac{1}{4}K^2)} \cosh \sqrt{(1+\tfrac{1}{4}K^2)}[L-Z] \\ & - \tfrac{1}{2}K \sinh \sqrt{(1+\tfrac{1}{4}K^2)}[L-Z]) / (\sqrt{(1+\tfrac{1}{4}K^2)} \\ & \cosh \sqrt{(1+\tfrac{1}{4}K^2)}L - \tfrac{1}{2}K \sinh \sqrt{(1+\tfrac{1}{4}K^2)}L) \} \end{aligned} \quad (12)$$

where V_{in} is the voltage at point of application.

A numerical example with $L=1.5$ and $K=-4.0$ in equations (11) and (12)

reveals that the voltage is attenuated at most by 97 and 26% from the initial voltage at the point of application, respectively. Therefore, the so-called asymmetry factor Ψ defined by Nitzen *et al.* (1990), believed to be equal to unity for a cylinder with sealed-ends (i.e. Neumann boundary conditions) is shown here to be $\Psi = 23$. Higher asymmetry factors could probably arise for transient solutions.

Results. The diameters and R_m values of dendritic segments at a large number of discrete electrotonic distances 0.05 apart were used to determine the profile of the equivalent dendritic cable governed by the factor F [see equation (9)]. The factor in Fig. 6 was approximated by an exponential function $\exp(-1.8Z)$ corresponding to the dashed line in Fig. 6.

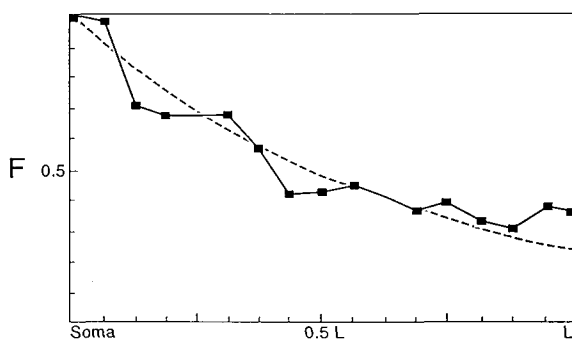


Figure 6. The electrogeometric ratio parameter (F) of the starburst amacrine cell plotted as a function of the electrotonic distance (Z) as calculated from the detailed geometry of the dendritic tree and assuming a non-uniform "sigmoidal" R_m distribution with a specific axial resistivity R_i of $300 \Omega\text{cm}$. The dashed curve represents an approximation of the parameter by an exponential function [$\exp(-1.8 Z)$].

The absence of information about the specific electrical membrane properties of rabbit starburst amacrine cells has resulted in the use of parameter values taken from amacrine cells from cold-blooded lower vertebrates (i.e. $R_i = 300 \Omega\text{cm}$, $R_{m,\text{soma}} = 1\,000 \Omega\text{cm}^2$ obtained by Nelson, 1973; and $R_{m,\text{max}} = 68\,000 \Omega\text{cm}^2$ obtained by Coleman and Miller, 1989). With these electrical parameters, the electrotonic length of 0.8 would imply that the starburst amacrine cells are electrotonically compact. Indeed, this has been verified from computations of the centripetal [see equation (11)] and centrifugal [see equation (12)] voltage decrement as shown in Fig. 7. In terms of voltage

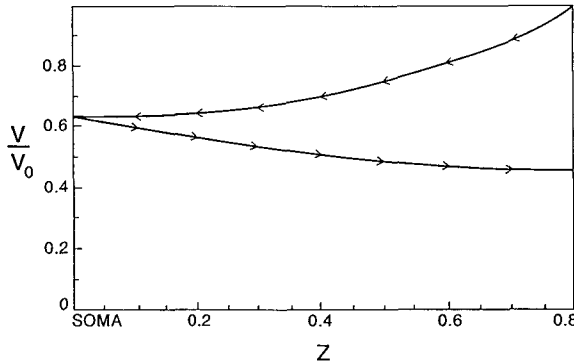


Figure 7. Centripetal and centrifugal attenuation of steady state voltage along a tapering (exponentially) equivalent cable model plotted as a function of electrotonic distance (Z) with $Z=0$ and $Z=0.8$ representing the soma and dendritic terminal, respectively. Arrowheads denote direction of current flow.

attenuation seen at the soma the result illustrates that synaptic potentials generated at the most distal dendritic sites would attenuate by only 37%, and by only 18% in the opposite direction. Therefore, even the most distal excitatory synaptic input activated on a certain dendrite is likely to have considerable influence on the activity of another dendrite.

A question that needs to be asked for the results to have any form of conviction is whether mammalian retinal neurons have electrical parameters that are as high as those in the amphibian retina. If the answer is no, then computations with lower R_m and R_i values need to be carried out. This can be accomplished by multiplying by a factor (different for each $R_{m,max}$ chosen) the electrotonic length measurement for each branch segment and also by changing the R_i value, whilst keeping the same l and d values in equation (1). The profile of the factor F (see Fig. 6) would remain the same except that the electrotonic length of the equivalent cable would be increased. For example, if $R_{m,max} = 4\,000\,\Omega\text{cm}^2$ and $R_i = 300\,\Omega\text{cm}$ then the electrotonic length would increase from 0.8 to 3.46. The results are presented in Fig. 8 by showing the tip-to-tip signal decrement measured as a percentage of voltage against a selection of $R_{m,max}$ values, with two particular R_i values chosen to represent the entire spectrum of possible R_i values. For example, if the spatial R_m distribution rises to $75\,000\,\Omega\text{cm}^2$ (i.e. $R_{m,max} = 75\,000\,\Omega\text{cm}^2$) then electrical transmission within the arbors of the starburst amacrine cell is quite good, with the voltage attenuation never exceeding about one-half. It is also important to note that with electrical parameter values originally assumed by Bloomfield and Miller (1983) (i.e. $R_{m,max} = 4000\,\Omega\text{cm}^2$, and $R_i = 70\,\Omega\text{cm}$), the results show the same voltage decrement as those predicted by Miller and Bloomfield (1983).

In terms of biological insight the purely theoretical results generated here may shed some light on the type of synaptic scheme (i.e. pre- or postsynaptic)

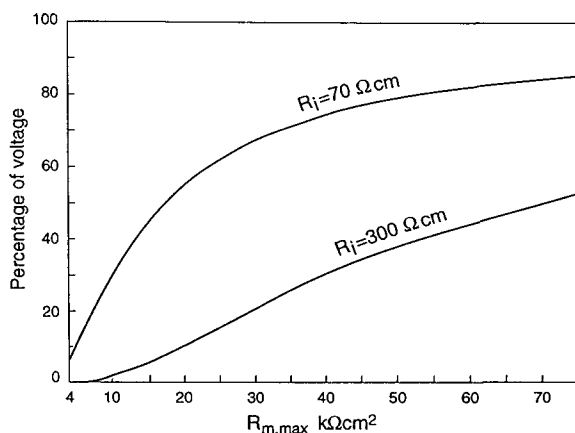


Figure 8. Tip-to-tip signal decrement along the starburst amacrine dendritic arbor shown as a percentage of voltage plotted against the maximum value of the spatially non-uniform R_m distribution for two different values of R_i shown labelled.

involved in retinal directional selectivity. If the electrical parameters for rabbit retinal neurons are found to be as high as those found in the amphibian retina then it would appear unlikely that dendritic isolation does exist putting doubt over the presynaptic scheme (see Masland and Tauchi, 1986), and thereby favouring a postsynaptic scheme (see Torre and Poggio, 1978; Poznanski, 1990). On the other hand, if the electrical parameters were found to be less than those assumed in this analysis then the probability of dendritic isolation occurring would be much greater. For example, if it was assumed that 90% was the maximum percentage of the signal decrement (or 10% residual transmission) that would allow the dendritic arbors of starburst amacrine cells to function autonomously then the results clearly show that $R_{m,max}$ would need to be under 5 000 and 20 000 Ωcm^2 for $R_i = 70$ and 300 Ωcm , respectively. For this particular choice of the membrane resistance value it can be seen from Fig. 9 that the terminal arborizations arising from each primary dendrite function in an autonomous manner.* More importantly, it is shown in Fig. 9 that dendrites of starburst amacrine cells process information with a bias towards the centrifugal direction. This observation is compatible with the result obtained by Famiglietti (1991) who claims that steady-state centripetal voltage attenuation is sevenfold while only threefold in the centrifugal direction. This asymmetric bi-directional current flow in starburst amacrine cells is a vital link in the recent presynaptic co-transmission model of retinal direction-selectivity proposed by Vaney (1990).

* It should be mentioned that any notion of dendritic isolation would appear very unlikely if the recent electrophysiological experiment performed by Bloomfield (1991) is to be taken into consideration. This is because a slit of light placed over the distal dendrites of a starburst amacrine cell generated a response detected at the cell body.

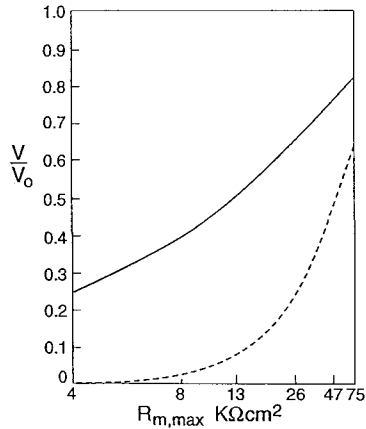


Figure 9. Centrifugal (—) and centripetal (---) attenuation of steady-state voltage along the starburst amacrine's dendritic arbor represented as an exponential equivalent dendrite having a specific axial resistivity (R_i) of $300 \Omega cm$ plotted against the maximum value of the spatially non-uniform "sigmoidal" membrane resistance (R_m) distribution.

Discussion. The classical concept of a neuron (see for example, Eccles, 1957) as a neural integrator of all incoming synaptic inputs (distributed on many dendrites) may apply to the starburst amacrine cells, but the concept of the axon as the sole output channel of the neuron cannot apply to the starburst amacrine cells, since they are axonless. Therefore various branch segments are more likely to be activated independently via dendrodendritic synapses as a result of a possible non-homogeneous input activated during directional visual stimulation. The symmetry requirement imposed on the cable model presented here allowed synaptic inputs to be distributed at *all* dendritic sites that were at equal electrotonic distance from the soma. This caveat in the theory of the equivalent cable model is difficult to dismiss when modelling a non-classical neuron (but see Rall and Rinzel, 1973; Redman, 1973; Rinzel and Rall, 1974).

Another assumption inherent in the cable model is the non-uniform R_m distribution. This assumption is a consequence of the possible non-uniform distribution of specific ion channels present in cat motoneurons and is not an intrinsic property of the neuronal membrane. As it appears unlikely that synaptic inputs are distributed uniformly over the dendritic membrane of starburst amacrine cells (Famiglietti, 1991), such a non-uniform synaptic input distribution could influence the way the specific membrane resistance is reduced during synaptic bombardments, but whether the starburst amacrine cells have a R_m distribution that follows a "sigmoidal" shape remains to be seen. Indeed, it may be that the difference between the input-output structure of starburst amacrine cells and other classical neurons warrants the use of other

forms of R_m distributions (e.g. the complement of the "sigmoidal" curve), but again this is left open for further investigation.

This work owes much to useful discussions with W. R. Levick and I. G. Morgan. I am grateful to D. I. Vaney for kindly providing the histological material on which this analysis was based and to D. Osorio for his advice on the photographic techniques.

LITERATURE

- Amthor, F. R., C. W. Oyster and E. S. Takahashi. 1984. Morphology of on-off direction-selective ganglion cells in the rabbit retina. *Brain Res.* **298**, 187–190.
- Ariel, M. and N. W. Daw. 1982. Pharmacological analysis of directionally sensitive rabbit retinal ganglion cells. *J. Physiol. (Lond.)* **324**, 161–185.
- Barlow, H. B. and R. M. Hill. 1963. Selective sensitivity to direction of movement in ganglion cells of the rabbit retina. *Science* **139**, 412–414.
- Barlow, H. B., R. M. Hill and W. R. Levick. 1964. Retinal ganglion cells responding selectively to direction and speed of image motion in the rabbit. *J. Physiol. (Lond.)* **173**, 377–407.
- Barlow, H. B. and W. R. Levick. 1965. The mechanism of directionally selective units in rabbit's retina. *J. Physiol. (Lond.)* **178**, 477–504.
- Borg-Graham, L. J. and N. M. Grzywacz. 1992. A model of the direction selectivity circuit in retina: transformations by neurons singly and in concert. In *Single Neuron Computation*, T. McKenna, J. Davis and S. F. Zornetzer (eds), pp. 347–375. Orlando, FL: Academic Press.
- Bloomfield, S. A. 1991. A comparison of receptive field and dendritic field sizes of amacrine cells in the rabbit retina. *Invest. Ophthalmol. Vis. Sci. Suppl.* **32**, 993.
- Brandon, C. 1987. Cholinergic neurons in the rabbit retina: dendritic branching and ultrastructural connectivity. *Brain Res.* **426**, 119–130.
- Brecha, N., D. Johnson, L. Peichl and H. Wässle. 1988. Cholinergic amacrine cells of rabbit retina contain glutamate decarboxylase and γ -aminobutyrate immunoreactivity. *Proc. natn. Acad. Sci. U.S.A.* **85**, 6187–6191.
- Caldwell, J. H., N. W. Daw and H. J. Wyatt. 1978. Effects of picrotoxin and strychnine on rabbit retinal ganglion cells: lateral interactions for cells with more complex receptive fields. *J. Physiol. (Lond.)* **276**, 277–298.
- Cole, K. S. 1968. *Membrane, Ions and Impulses: A Chapter of Classical Biophysics*. Berkeley, CA: California University Press.
- Coleman, P. A. and R. F. Miller. 1989. Measurements of passive membrane parameters with whole-cell recording from neurons in the intact amphibian retina. *J. Neurophysiol.* **61**, 218–230.
- Dowling, J. E. 1968. Synaptic organization of the frog retina: an electron microscopic analysis comparing the retinas of frogs and primates. *Proc. R. Soc. (Lond.) B* **170**, 205–228.
- Dowling, J. E. 1970. Organization of vertebrate retinas. *Invest. Ophthalmol.* **9**, 655–680.
- Dowling, J. E. 1987. *The Retina: An Approachable Part of the Brain*. Cambridge, MA: Harvard University Press.
- Dowling, J. E. and F. S. Werblin. 1969. Organization of the retina of the mudpuppy. I. Synaptic structure. *J. Neurophysiol.* **32**, 315–338.
- Eccles, J. C. 1957. *The Physiology of Nerve Cells*. Baltimore: John Hopkins Press.
- Famiglietti, E. V. 1983a. 'Starburst' amacrine cells and cholinergic neurons: mirror-symmetric ON and OFF amacrine cells of rabbit retina. *Brain Res.* **261**, 138–144.
- Famiglietti, E. V. 1983b. On and off pathways through amacrine cells in mammalian retina: the synaptic connections of 'starburst' amacrine cells. *Vision Res.* **23**, 1265–1279.

- Famiglietti, E. V. 1985. Synaptic organization of on-off directionally selective ganglion cells in rabbit retina. *Soc. Neurosci. Abstr.* **1**, 337.
- Famiglietti, E. V. 1991. Synaptic organization of starburst amacrine cells in rabbit retina: analysis of serial thin sections by electron microscopy and graphic reconstruction. *J. Comp. Neurol.* **309**, 40–70.
- Fleshman, J. W., I. Segev and R. E. Burke. 1988. Electrotonic architecture of type-identified α -motoneurons in the cat spinal cord. *J. Neurophysiol.* **60**, 60–85.
- Glenn, L. L. 1988. Overestimation of the electrical length of neuron dendrites and synaptic electrotonic attenuation. *Neurosci. Lett.* **91**, 112–119.
- Hines, M. 1989. A program for simulation of nerve equations with branching geometries. *Int. J. Biomed. Comput.* **24**, 55–68.
- Holmes, W. R. and C. D. Woody. 1989. Effects of uniform and non-uniform synaptic 'activation-distributions' on the cable properties of modeled cortical pyramidal neurons. *Brain Res.* **505**, 12–22.
- Goldstein, S. S. and W. Rall. 1974. Changes of action potential shape and velocity for changing core conductor geometry. *Biophys. J.* **14**, 731–757.
- Jack, J. J. B., D. Noble and R. W. Tsien. 1975. *Electric Current Flow in Excitable Cells*. Oxford: Clarendon Press.
- Leibovic, K. N. 1972. *Nervous System Theory: An Introductory Study*. New York: Academic Press.
- Maranto, A. R. 1982. Neuronal mapping: a photooxidation reaction makes Lucifer yellow useful for electron microscopy. *Science* **217**, 953–955.
- Masland, R. H. and A. Ames. 1976. Responses to acetylcholine of ganglion cells in an isolated mammalian retina. *J. Neurophysiol.* **39**, 1220–1235.
- Masland, R. H. and M. Tauchi. 1986. The cholinergic amacrine cell. *Trends Neurosci.* **9**, 218–223.
- Massey, S. C. and M. J. Neal. 1979. The light-evoked release of acetylcholine from the rabbit retina in vivo and its inhibition by gamma-aminobutyric acid. *J. Neurochem.* **32**, 1327–1329.
- Massey, S. C. and D. A. Redburn. 1982. A tonic gamma-aminobutyric acid-mediated inhibition of cholinergic amacrine cells in rabbit retina. *J. Neurosci.* **2**, 1633–1643.
- Millar, T. J. and I. G. Morgan. 1987. Cholinergic amacrine cells in the rabbit retina synapse onto other cholinergic amacrine cells. *Neurosci. Lett.* **74**, 281–285.
- Miller, R. F. and S. A. Bloomfield. 1983. Electroanatomy of a unique amacrine cell in the rabbit retina. *Proc. natn. Acad. Sci. U.S.A.* **80**, 3069–3073.
- Morgan, I. G. and Z.-K. Li. 1990. Are there GABA_a receptors on cholinergic amacrine cells? *Proc. Aust. Neurosci. Soc.* **1**, 111.
- Neal, M. J. and S. C. Massey. 1980. The release of acetylcholine and amino acids from the rabbit retina in vivo. *Neurochemistry* **1**, 191–208.
- Nelson, R. 1973. A comparison of electrical properties of neurons in Necturus retina. *J. Neurophysiol.* **36**, 519–535.
- Nitzan, R., I. Segev and Y. Yarom. 1990. Voltage behavior along the irregular dendritic structure of morphologically and physiologically characterized vagal motoneurons in the guinea pig. *J. Neurophysiol.* **63**, 333–346.
- O'Malley, D. M. and R. H. Masland. 1989. Co-release of acetylcholine and γ -aminobutyric acid by a retinal neuron. *Proc. natn. Acad. Sci. U.S.A.* **86**, 3414–3418.
- Oyster, C. W. 1968. The analysis of image motion by the rabbit retina. *J. Physiol. (Lond.)* **199**, 613–635.
- Oyster, C. W. 1989. Neural interactions underlying direction-selectivity in the rabbit retina. In *Vision: Coding and Efficiency*, C. Blakemore (Ed.), pp. 92–102. New York: Cambridge University Press.
- Oyster, C. W. and H. B. Barlow. 1967. Direction-selective units in rabbit retina: distribution of preferred directions. *Science* **155**, 841–842.
- Pongracz, F., S. Firestein and G. M. Shepherd. 1991. Electrotonic structure of olfactory sensory

- neurons analyzed by intracellular and whole cell patch techniques. *J. Neurophysiol.* **65**, 747–758.
- Poznanski, R. R. 1988. Membrane voltage changes in passive dendritic trees: a tapering equivalent cylinder model. *IMA J. Math. appl. Med. Biol.* **5**, 113–145.
- Poznanski, R. R. 1990. Analysis of a postsynaptic scheme based on a tapering equivalent cable model. *IMA J. Math. appl. Med. Biol.* **7**, 175–197.
- Poznanski, R. R. 1991. A generalized tapering equivalent cable model for dendritic neurons. *Bull. math. Biol.* **53**, 457–467.
- Rall, W. 1959. Branching dendritic trees and motoneuron membrane resistivity. *Exp. Neurol.* **1**, 491–527.
- Rall, W. 1962. Theory of physiological properties of dendrites. *Ann. N.Y. Acad. Sci.* **96**, 1071–1092.
- Rall, W. 1982. Theoretical models which increase R_m with dendritic distance help fit lower value of C_m . *Soc. Neurosci. Abstr.* **8**, 414.
- Rall, W. 1990. Perspectives on neuron modeling. In *The Segmental Motor System*, M. D. Binder and L. M. Mendell (Eds), pp. 129–149. Oxford: Oxford University Press.
- Rall, W. and J. Rinzel. 1973. Branch input resistance and steady attenuation for input to one branch of a dendritic neuron model. *Biophys. J.* **13**, 648–688.
- Redman, S. J. 1973. The attenuation of passively propagating dendritic potentials in a motoneurone cable model. *J. Physiol. (Lond.)* **234**, 637–664.
- Redman, S. J., E. M. McLachlan and G. D. S. Hirst. 1987. Nonuniform passive membrane properties of rat lumbar sympathetic ganglion cells. *J. Neurophysiol.* **57**, 633–644.
- Rinzel, J. and W. Rall. 1974. Transient response in a dendritic neuron model for current injected at one branch. *Biophys. J.* **14**, 759–790.
- Tauchi, M. and R. H. Masland. 1984. The shape and arrangement of the cholinergic neurons in the rabbit retina. *Proc. R. Soc. (Lond.) B* **223**, 101–119.
- Torre, V. and T. Poggio. 1978. A synaptic mechanism possibly underlying directional selectivity to motion. *Proc. R. Soc. (Lond.) B* **202**, 409–416.
- Tsien, R. Y. 1989. Fluorescent probes of cell signalling. *Ann. Rev. Neurosci.* **12**, 227–253.
- Vaney, D. I. 1984. ‘Coronate’ amacrine cells in the rabbit retina have the ‘starburst’ dendritic morphology. *Proc. R. Soc. (Lond.) B* **220**, 501–508.
- Vaney, D. I. 1985. Fireworks in the retina. *Nature* **314**, 672–673.
- Vaney, D. I. 1990. The mosaic of amacrine cells in the mammalian retina. In *Progress in Retinal Research*, Vol. 9, N. Osborne and J. Chader (Eds), pp. 49–100. Oxford: Pergamon Press.
- Vaney, D. I. and H. M. Young. 1988. GABA like immunoreactivity in cholinergic amacrine cells of the rabbit retina. *Brain Res.* **438**, 369–373.
- Vaney, D. I., S. P. Collins and H. M. Young. 1989. Dendritic relationships between cholinergic amacrine cells and direction selective retinal ganglion cells. In *Neurobiology of the Inner Retina*, NATO ASI Series, Vol. H31, R. Weiler and N. N. Osborne (Eds), pp. 157–168. Berlin: Springer-Verlag.
- Wassle, H. and B. B. Boycott. 1991. Functional architecture of the mammalian retina. *Physiol. Rev.* **71**, 447–479.
- Wyatt, H. J. and N. W. Daw. 1975. Directionally sensitive ganglion cells in the rabbit retina: specificity for stimulus direction, size, and speed. *J. Neurophysiol.* **38**, 613–626.
- Wyatt, H. J. and N. W. Daw. 1976. Specific effects of neurotransmitter antagonists on ganglion cells in rabbit retina. *Science* **191**, 204–205.

Received 15 May 1991

Revised 3 November 1991